Journal of Experimental & Clinical Cancer Research

RESEARCH Open Access

Ethaselen synergizes with oxaliplatin in tumor growth inhibition by inducing ROS production and inhibiting TrxR1 activity in gastric cancer

Haiyong Zhang[1,2†], Jing Wu[1†], Jinqiu Yuan[3†], Huafu Li[1,2], Yawei Zhang[1,2], Wang Wu[1,2], Wei Chen[4], Chunming Wang[1,2], Sijun Meng[1], Songyao Chen[1], Mingyu Huo[1*], Yulong He[1,2*] and Changhua Zhang[1,2*]

Abstract

Background: Oxaliplatin is one of the most commonly used chemotherapeutic agent for the treatment of various cancers, including gastric cancer. It has, however, a narrow therapeutic index due to its toxicity and the occurrence of drug resistance. Hence, it is of great significance to develop novel therapies to potentiate the anti-tumor effect and reduce the toxicity of oxaliplatin. In our previous study, we demonstrated that ethaselen (BBSKE), an inhibitor of thioredoxin reductase, effectively inhibited the growth of gastric cancer cells and promoted apoptosis in vitro. In the present study, we investigated whether BBSKE can potentiate the anti-tumor effect of oxaliplatin in gastric cancer in vivo and vitro.

Methods: Cellular apoptosis and ROS levels were analyzed by flow cytometry. Thioredoxin reductase 1 (TrxR1) activity in gastric cancer cells, organoid and tumor tissues was determined by using the endpoint insulin reduction assay. Western blot was used to analyze the expressions of the indicated proteins. Nude mice xenograft models were used to test the effects of BBSKE and oxaliplatin combinations on gastric cancer cell growth in vivo. In addition, we also used the combined treatment of BBSKE and oxaliplatin in three cases of gastric cancer Patient-Derived organoid (GC-PDO) to detect the anti-tumor effect.

Results: We found that BBSKE significantly enhanced oxaliplatin-induced growth inhibition in gastric cancer cells by inhibiting TrxR1 activity. Because of the inhibition of TrxR1 activity, BBSKE synergized with oxaliplatin to enhance the production of ROS and activate p38 and JNK signaling pathways which eventually induced apoptosis of gastric cancer cells. In vivo, we also found that BBSKE synergized with oxaliplatin to suppress the gastric cancer tumor growth in xenograft nude mice model, accompanied by the reduced TrxR1 activity. Remarkably, we found that BBSKE attenuated body weight loss evoked by oxaliplatin treatment. We also used three cases of GC-PDO and found that the combined treatment of BBSKE and oxaliplatin dramatically inhibited the growth and viability of GC-PDO with increased ROS level, decreased TrxR1 activity and enhanced apoptosis.

* Correspondence: mingyu9318@163.com; heyulong@mail.sysu.edu.cn; zhchangh@mail.sysu.edu.cn
†Haiyong Zhang, Jing Wu, Jinqiu Yuan contributed equally to this work.
[1]Digestive Diseases Center, The Seventh Affiliated Hospital, Sun Yat-sen University, 518107 Shenzhen, Guangdong, China
Full list of author information is available at the end of the article

Conclusions: This study elucidates the underlying mechanisms of synergistic effect of BBSKE and oxaliplatin, and suggests that the combined treatment has potential value in gastric cancer therapy.

Keywords: Tumor growth inhibition, Thioredoxin reductase 1, Reactive oxygen species, Ethaselen, Oxaliplatin, Organoids, Gastric cancer

Background

Gastric cancer is the main cause of cancer-related deaths in the world [1, 2]. Although surgical resection may be curative in early stages of the disease, chemotherapy still remains the cornerstone for the treatment of patients diagnosed with advanced stages [3, 4]. Oxaliplatin is a potent chemotherapeutic agent that is widely used for the treatment of various cancers including gastric cancer[5, 6].However, the clinical application of oxaliplatin is limited due to drug resistance and side effects [7, 8]. Adjuvant chemotherapy have been prescribed for gastric cancer and have shown considerable benefits in reducing cancer recurrence and increasing long-term survival [9, 10]. Hence, it is of great significance to develop new agents to synergize with oxaliplatin and decrease side effects.

Thioredoxin reductase 1 (TrxR1) is a selenocysteine (Sec) containing flavoenzyme that plays a critical role in regulating intracellular redox balances [11]. TrxR1 has been found to be up-regulated in a variety of human tumors and to be associated with increased tumor growth, drug resistance and a poor patient outcome [12, 13]. Moreover, it has been found that TrxR1 inactivation by chemical inhibitors may reverse tumor growth and sensitize cancer cells to chemotherapeutic drugs, suggesting that TrxR1 may serve as an attractive therapeutic target for anticancer drug development [14–17]. Based on this notion, the development of novel inhibitors of TrxR1 as potential antitumor agents has gained attention during recent years [18–20].

The challenge of translating novel treatment regimens from bench to bedside is mainly due to the fact that many cancer models poorly simulate the in vivo condition, and as a consequence, many drugs that perform well in cancer models ultimately fail in clinical trials [21]. Organoids are three-dimensional ex vivo models that can accurately simulate in-vitro conditions and can be cultured efficiently using human tissue [22]. Recently, organoid has also been shown to be a good model to determine the optimal drugs for the patients [23–27]. Using organoid models to study the behavior of malignant cells and their interactions with the microenvironment is a hot area of research [28].

Ethaselen (BBSKE), an inhibitor of thioredoxin reductase, is known to selectively kill cancer cells and many studies have suggested that BBSKE can interact with TrxR1 both in vitro and in vivo [29]. By inhibiting TrxR1 activity and increasing intracellular ROS, BBSKE induces a lethal endoplasmic reticulum stress and mitochondrial dysfunction in human gastric cancer cells [30].

We have successfully established and passaged GC-PDO, and verified the consistency of these organs with the primary carcinoma tissue through histopathological examination [31]. Our previous study has suggested that BBSKE induced growth inhibition and apoptosis in gastric cancer cells and GC Patient-Derived organoid [32]. In the present study, we investigated whether BBSKE could synergize to enhance the anti-tumor effects of oxaliplatin in gastric cancer cells and GC-PDO. We found that BBSKE significantly enhanced oxaliplatin-induced growth inhibition of these cells and GC-PDO. TrxR1 activity is involved in their synergistic effect both in vitro and in vivo. Our data elucidated the underlying mechanisms of synergistic activity of BBSKE and oxaliplatin, and suggest that such a combination treatment might potentially become a more effective regimen in gastric cancer therapy.

Materials and methods

Cell culture and reagents

BBSKE was synthesized and provided by the Department of Chem-Biology, School of Pharmaceutical Sciences, Peking University, China. BBSKE was stored as a 20 mmol/L solution in absolute DMSO at -20 °C, and diluted with the medium prior to use. The final concentration of DMSO in medium is maximum 0.25 %. Human gastric cancer cell lines SGC-7901, MGC-803 and gastric cell lines GES-1 were purchased from the Institute of Biochemistry and Cell Biology, Chinese Academy of Sciences. The cells were routinely cultured in RPMI1640 (Gibco, Eggenstein, Germany) containing 10 % heat-inactivated fetal bovine serum (Gibco, Eggenstein, Germany), 100 units/mL penicillin, and 100 μg/mL streptomycin in a humidified cell incubator with an atmosphere of 5 %CO2 at 37℃. N-acetyl-L-cysteine (NAC), L-glutathione (GSH) and cisplatin were purchased from Sigma (St. Louis, MO, USA). The matrigel was purchased from USA. Antibodies including anti-Bcl-2 (sc-7382, 1:50), anti-TrxR1 (sc-28,321, 1:200), anti-GAPDH (sc-47,724, 1:200), mouse anti-rabbit IgG-HRP (sc-2357, 1:2000) and m-IgGκ BP-HRP (sc-516,102, 1:2000) were purchased from Santa Cruz Biotechnology (Santa Cruz, CA, USA). Antibodies including anti-p-p38 (4631, 1:1000), anti-p38 (9212, 1:1000), anti-p-JNK

(4668, 1:1000) and anti-JNK (9252, 1:1000) were purchased from Cell Signaling Technology (Danvers, MA, USA). The anti-Ki-67 (ab15580, 1:1000) antibody was purchased from Abcam (Cambridge, MA, USA). FITC Annexin V apoptosis Detection Kit I and Propidium Iodide (PI) were purchased from BD Pharmingen (Franklin Lakes, NJ, USA).

Cells and organoids viability assay

Cells were seeded into 96-well culture plates at a density of 5 × 103 per well for 24 h. After indicated treatments, cell viability was examined by Cell Counting Kit-8 (CCK8, Dojindo, Japan). The combination index (CI) of drug interaction was determined using the Chou-Talalay method [33]: CI = 1, additive interaction; CI > 1, antagonistic interaction; and CI < 1, synergistic interaction.

Measurement of intracellular ROS

Cells and organoids were seeded into 6-well culture plates for 24 h, and then treated with BBSKE, oxaliplatin, or the combination for 2 h. Cells were stained with 10 μM DCFH-DA (Beyotime Biotech, Nantong, China) for 30 min. Then the cells were collected and the fluorescence intensity was analyzed using a Flex Flow Cytometer (Beckman Coulter, Brea, CA, USA). In some experiments, cells were pretreated with 5 mM NAC (ROS inhibitor) or GSH for 2 h prior exposure to compounds.

Cells and organoids apoptosis analysis

Cells and organoids were seeded into 6-well culture plates for 24 h, and then treated with BBSKE, oxaliplatin, or the combination for 24 h. Then the cells were harvested, washed twice with ice-cold phosphate-buffered saline (PBS), and evaluated for apoptosis by double staining with annexin V-FITC and propidium iodide in binding buffer for 30 min using a Flex Flow Cytometer (Beckman Coulter, Brea, CA, USA).

Western blot analysis

Cells were grown on 6-well culture plates and were treated with BBSKE, oxaliplatin, or the combination for the indicated times. The cells were then washed twice or three times with 1 mL of PBS, and were lysed using cell lysis buffer. For western blot analysis, equal amounts of protein in each sample were separated by sodium dodecyl sulfate-polyacrylamide gel electrophoresis and electroblotted onto polyvinylidene difluoride membrane. The membranes were blocked using 5 % nonfat milk at room temperature for 1 h and then incubated with primary antibodies at 4 °C overnight. Then, the membranes were washed three times with TBST for 10 min each time, and incubated with the peroxidase-conjugated secondary antibodies for 1 h at room temperature. The immunoreactive bands were visualized using an ECL detection kit (Bio-Rad Laboratories, CA, USA) and the images were captured and analyzed with the ChemiDoc Imaging Systems.

Patients' information and tissue samples

This study was approved by the Institutional Research Human Ethical Committee of the Seventh Affiliated Hospital of Sun Yat-Sen University for the use of clinical specimens and informed consents were obtained from all the patients. A total of 3 gastric cancer patients that were clinically diagnosed at the Seventh Affiliated Hospital of Sun Yat-sen University during the period of 2018 to 2019 were included. Gastric cancer tissues and the matched tumor-adjacent morphologically normal gastric tissues were frozen and stored in liquid nitrogen for further use.

Patient-derived-Organoids culture

Gastric cancer tissues were instantly obtained after resected from GC patients. Tumor tissues were kept in Dulbecco's Phosphate Buffered Saline (DPBS)without Ca2 + and Mg2 + and supplemented with antibiotics. Then tissues were minced into pieces of 1–3 mm3 in size. The tissues were then digested in 10 mL GC organoid medium containing 1–2 mg/mL collagenase (Sigma, C9407) on an orbital shaker at 37 °C for 1–2 h. Then the acquired tissue suspension was sequentially sheared using 10 mL and 5mL plastic and flamed glass Pasteur pipettes. After every shearing the suspension was strained over a 100 μm filter with retained tissue pieces entering a subsequent shearing step with 10mL AdDF+++ (Advanced DMEM/F12 containing 1x Glutamax, 10 mM HEPES, and antibiotics) centrifugation at 300 rcf. The resuspension was mixed with Matrigel at the ratio of 2: 1. The mixed liquid was dropped into prewarmed 6-well suspension culture plates with each drop of 40 μL and gelatinized in an incubator at 37℃ for 10 min. Then the plates were transferred to humidified 37 °C/5 % CO2 incubators after 1.5 mL IntestiCult Organoid Growth Medium (Stemcell, 06010) added to each well. Organoids were observed and images were captured using a microscope (Leica DM4, Germany).

Docking of BBSKE to the TrxR1 structural model

To study the interaction between the BBSKE and TrxR1, a protein-molecular docking was implemented by ChemBioDraw module and Schrodinger 2018 software. The crystal structure of human TrxR1 (PDB code:3ean) was used for present docking study. The water molecules, the original ligand molecules and their non-related protein conformation in the crystal structure of the protein were deleted. After being processed by the Clean Protein tool, the OPLS2005 force field was added to optimize

the energy. With the original ligand position as the center, the residues within the 18 angstrom range were selected as the docking pocket. The planar structure of the compound (Additional file 1: Figure S1) to be docked was mapped in Chemdraw. In Schrodinger, the ligand preparation module was used to optimize the structure of the ligand, and OPLS2005 was used for the force field. In Schrodinger, XP (Extra Precision) docking mode was used to dock the prepared ligand with the receptor. The default parameters were used for running the docking simulation.

TrxR1 activity measurement in cells, organoid and tumor tissues

Cells were grown in 6-well culture plates and treated with BBSKE, oxaliplatin, or the combination for the indicated times. Next, the cells were lysed with lysis buffer and protein concentrations were determined using the Bradford assay. TrxR1 activity in cell lysates or tumor tissues was determined using an endpoint insulin reduction assay [34]. Briefly, cell extracts containing 100 μg total protein were incubated in a final reaction volume of 50 μL containing 0.3 mM insulin, 100 mM Tris-HCl (pH 7.6), 3 mM EDTA, 660 μM NADPH, and 15 μM E. coli Trx (Sigma, St. Louis, MO) for 30 min. The reactions were terminated by adding 200 μL 1 mM DTNB in 6 M guanidine hydrochloride (pH 8.0). A blank control sample (containing everything except Trx) was treated in the same manner. The absorbance was measured using a SpectraMax iD3 microplate reader (Molecular Devices, USA) at 412 nm, and the activity was expressed as percentage of the blank control.

In vivo antitumor study

Male BALB/c nude mice (3–4 weeks of age) were housed in specific pathogen-free facilities. The protocols involving animals were approved by the Institutional Ethics Committee for Clinical Research and Animal Trials of the Seven Affiliated Hospital, Sun Yat-sen University. The mice were injected subcutaneously with 5×106 MGC-803 cells. When tumors reached a size of 5–6 mm in diameter, they were randomly divided into a control group and treatment groups including BBSKE alone, oxaliplatin alone and BBSKE in combination with oxaliplatin (6 mice per group). The sample size was based on our extensive experience in analyzing mouse xenografts. No animals were excluded from the analysis. The investigators were not blinded to group allocation. BBSKE or solvent (0.5 % sodium carboxymethyl cellulose, CMC-Na) were administered by intragastric (i.g.), at a dose of 36 mg per kg, per day. Oxaliplatin was administered by intraperitoneal (i.p.) injection at 5 mg per kg per week. At the end of experiment, the mice were euthanized and some organs were excised and weighed. Tumor volume= (π/6) (W2) (L), where W represents width, and L represents length.

Immunohistochemistry assay

The harvested tumor tissues were fixed in 4 % paraformaldehyde for 24 h. Fixed tissues were embedded in paraffin and cut into 5-μm sections. Tissue sections were stained with the indicated antibodies. The signal was detected by biotinylated secondary antibodies, and color was developed using DAB (3,3′-diaminobenzidine).

Statistical analysis

All experiments were performed in triplicate. The data are reported as means ± SEM. All statistical analyses were performed using GraphPad Prism 7.0. Student's t-test and two-way ANOVA were employed to analyze the differences between data sets. A p value < 0.05 was considered statistically significant.

Results

BBSKE synergistically augmented the cytotoxicity of oxaliplatin in gastric cancer cells

To determine whether BBSKE can synergize with oxaliplatin to kill cancer cells, we first tested the effect of BBSKE or oxaliplatin alone or their combination on the viability of SGC-7901 and MGC-803 cells. Using a CCK8 assay, we found BBSKE treatment suppressed the growth of gastric cancer cells in a dose-dependent manner (Additional file 1: Figure S2A). In addition, we found 5 μM BBSKE significantly increased the cytotoxicity of oxaliplatin in SGC-7901 and MGC-803 cells (Fig. 1a-b) but showed no cytotoxic effect on GES-1 cell (Additional file 1: Figure S2B). The interaction of BBSKE and oxaliplatin was calculated by using combination index values (Fig. 1c-d), which demonstrated that BBSKE in combination with oxaliplatin exhibited a synergistic effect in gastric cancer cells. Furthermore, compared with BBSKE or oxaliplatin treatment alone, the combined treatment dramatically increased the apoptotic cell death in both SGC-7901 and MGC-803 cells (Fig. 1e-f). These results suggested that BBSKE synergized the chemotherapeutic effect of oxaliplatin in gastric cancer cells.

BBSKE and oxaliplatin cooperated to trigger ROS-dependent apoptosis in gastric cancer cells

The current study showed that BBSKE in combination with oxaliplatin exhibited a synergistic effect in SGC-7901 and MGC-803 cells. Hence, it is of great significance to investigate the synergistic mechanisms of BBSKE and oxaliplatin. Previous studies have suggested that intracellular ROS generation plays an important role in various anticancer agents-induced cancer cell apoptosis [35–37]. Moreover, current evidences showed that BBSKE can increase ROS level in cancer cells, which

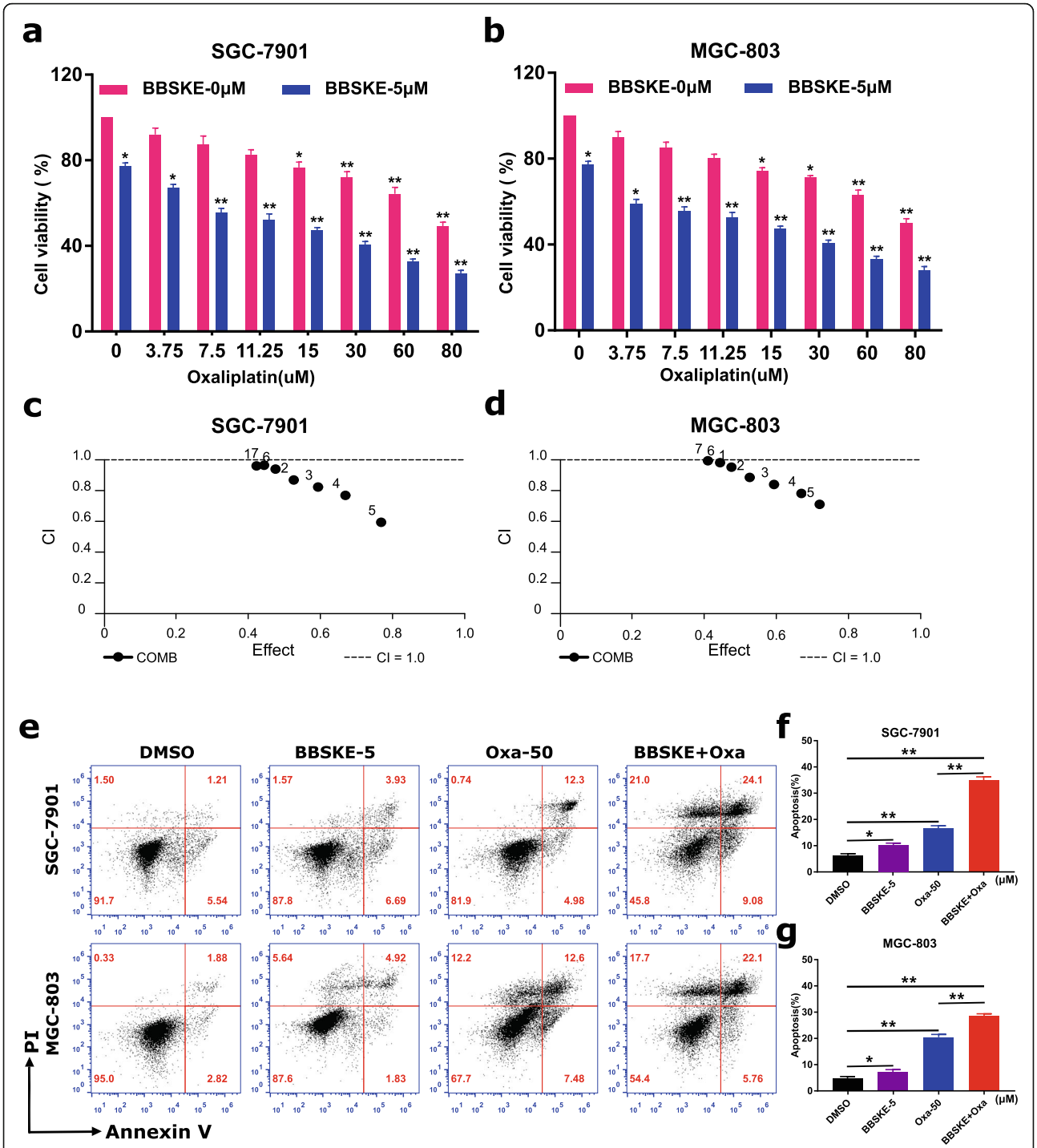

Fig. 1 BBSKE synergistically increased the cytotoxicity of oxaliplatin in gastric cancer cells. **a-b** SGC-7901 and MGC-803 cells were treated with BBSKE and oxaliplatin alone or in combination with the indicated concentrations. At 24 h after treatment, the cell viability was determined by CCK8 assay. **c-d** The combination index (CI) values of BBSKE combined with oxaliplatin were calculated using the calcusyn software. **e-g** SGC-7901 and MGC-803 cells were treated with BBSKE and oxaliplatin alone or in combination with the indicated concentrations. At 24 h after treatment, the percentage of cell apoptosis was determined by Annexin-V/PI staining and flow cytometry, and the percentage of apoptotic cells in the treatment groups was calculated. (* $p < 0.05$, ** $p < 0.01$)

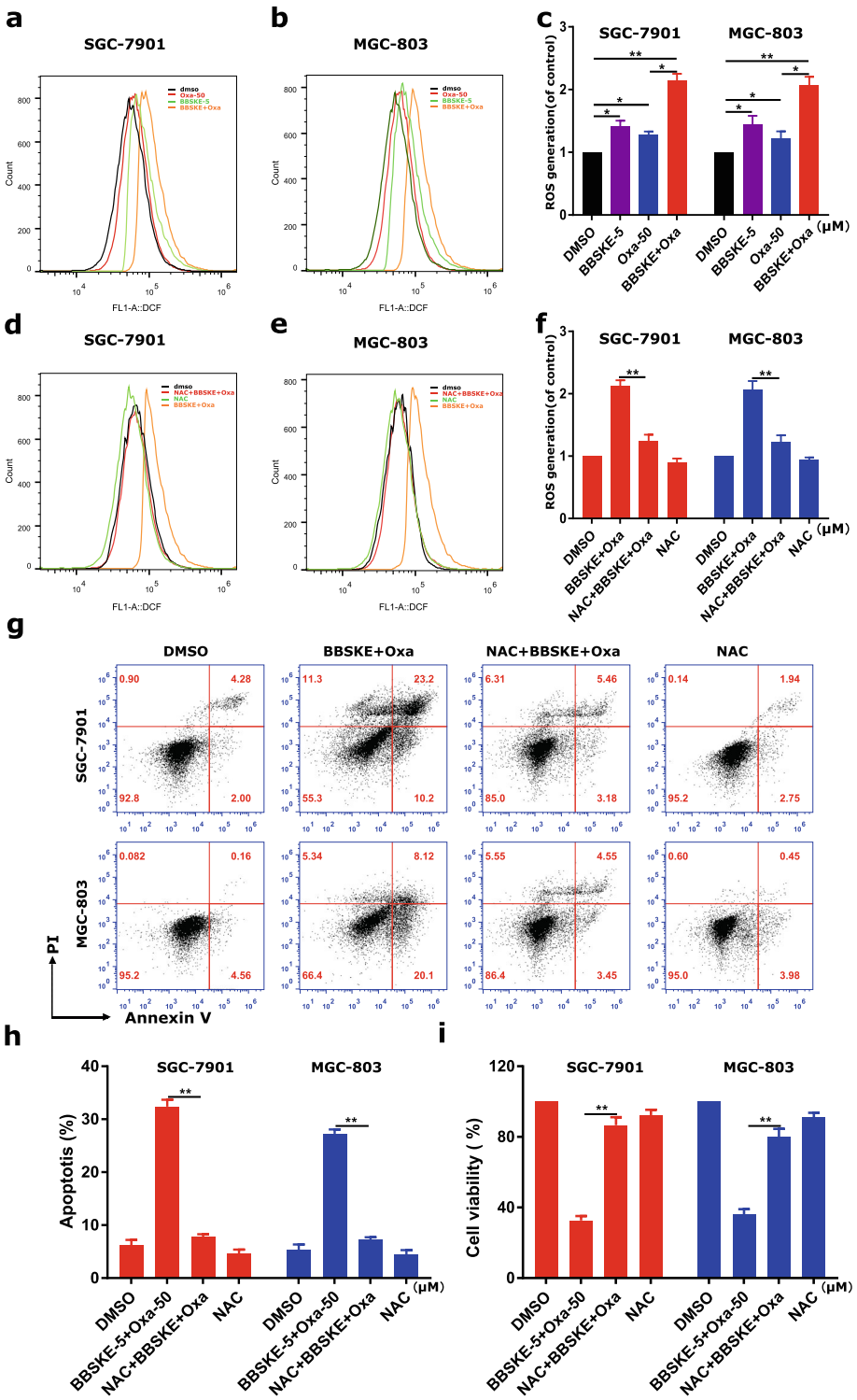

Fig. 2 (See legend on next page.)

(See figure on previous page.)
Fig. 2 BBSKE cooperated with oxaliplatin in inducing ROS-dependent apoptosis in gastric cancer cells. **a-c** SGC-7901 and MGC-803 cells were treated with BBSKE and oxaliplatin alone or in combination with the indicated concentrations. At 2 h after treatment, intracellular ROS generation was determined by flow cytometry. **d-f** SGC-7901 and MGC-803 cells were pretreated with 5 mM NAC for 2 h before the combined treatment of BBSKE and oxaliplatin. Intracellular ROS generation was measured by flow cytometry. **g-h** SGC-7901 and MGC-803 cells were pretreated with 5 mM NAC for 2 h before treated with BBSKE and oxaliplatin for 24 h. The percentage of cell apoptosis was determined by flow cytometry and the percentage of apoptotic cells was analyzed. **i** SGC-7901 and MGC-803 cells were pretreated with 5 mM NAC for 2 h before the combined treatment of BBSKE and oxaliplatin. At 24 h after treatment, the cell viability was determined by CCK8 assay. Data represent similar results from three independent experiments. (* $p < 0.05$, ** $p < 0.01$)

may underlie its cancer cell-killing activity [30]. To study whether ROS was involved in the synergistic effect, we detected the intracellular ROS level in gastric cancer cells treated with BBSKE and oxaliplatin alone or in combination. As shown in Fig. 2a-c, cells treated with BBSKE and oxaliplatin alone showed increased ROS generation, and the combined treatment further induced higher level of ROS. In addition, we found that pretreatment with NAC markedly reversed the combined treatment-induced increase in ROS level (Fig. 2d-f) which suggested that ROS accumulation is a necessary event in the synergistic effect. We also found that the combined treatment-induced apoptosis was significantly abrogated by NAC (Fig. 2 g-h). We additionally found that scavenging of ROS significantly attenuated the combined treatment-induced growth inhibition in both SGC-7901 and MGC-803 cells by using CCK8 assay (Fig. 2i and Additional file 1: Figure S3). These results revealed the vital role of ROS in the synergistic effect of BBSKE and oxaliplatin.

BBSKE and oxaliplatin combination activated ROS-mediated p38 and JNK signaling pathways

In response to ROS, the oxidized thioredoxin (Trx) form is released and activates ASK1 to mediate apoptosis via the p38 and JNK signaling pathways [38, 39]. Therefore, we hypothesized that the activation of p38 and JNK signaling pathways contributes to combined treatment-induced gastric cancer cells apoptosis. The results demonstrated that BBSKE or oxaliplatin treatment alone can activate the phosphorylation of p38 and JNK in both SGC-7901 and MGC-803 cells (Fig. 3a-b), and the combined treatment resulted in more significant increases of the phosphorylation levels of p38 and JNK in time-dependent manner (Fig. 3a-d). To further validate the involvement of the p38 and JNK signaling pathways in BBSKE and oxaliplatin-mediated cell growth inhibition and apoptosis, the SGC-7901 and MGC-803 cells were co-treated with BBSKE and oxaliplatin after pretreatment with p38 inhibitor BMS-582,949 or JNK inhibitor SP600125. We found that pretreatment with BMS-582,949 or SP600125 markedly reversed the combined treatment-induced phosphorylation of p38 or JNK in SGC-7901 cells (Additional file 1: Figure S4). Moreover, we found that BMS-582,949 or SP600125 can partially attenuate combined treatment-induced cell growth inhibition and apoptosis (Fig. 3e-f), suggesting that the activation of p38 and JNK signaling pathways is essential for the lethality of combined treatment.

Furthermore, we used ROS inhibitor (NAC) to detect the roles of ROS in the activation of p38 and JNK signaling pathways. We found that pretreatment with NAC markedly reversed the combined treatment-induced phosphorylation of p38 and JNK in both SGC-7901 and MGC-803 cells (Fig. 4a-d). Taken together, these results suggested that the activation of p38 and JNK signaling pathways was mainly due to accumulation of intracellular ROS in gastric cancer cells.

BBSKE and oxaliplatin combination inhibits TrxR1 activity in gastric cancer cells

TrxR1 is an important regulator of the redox balance in cells and accumulating evidence indicates that the intracellular level of ROS may increase when TrxR1 activity is inhibited [34, 40, 41]. To detect whether TrxR1 is involved in the synergistic effect, we first performed a molecular simulation of BBSKE-TrxR1 complex using docking software. BBSKE falls nicely into the TrxR1's pocket and its two carbonyl groups form hydrogen bonds with the residues ALA198 and ARG221 respectively (Additional file 1: Figure S5A-S5B). Additionally, the TrxR1 activity was measured by using an endpoint insulin reduction assay and we found that TrxR1 activity in SGC-7901 and MGC-803 cell lysates was inhibited by BBSKE and oxaliplatin respectively in dose dependent (Fig. 5a-b). While the combined treatment of BBSKE and oxaliplatin exerted a stronger inhibitory effect on TrxR1 activity in both SGC-7901 and MGC-803 cells (Fig. 5c-d). The western blot analysis showed that the level of TrxR1 had no significant change after treatment with BBSKE and oxaliplatin alone or in combination (Fig. 5e-f). These results indicated that the effects of BBSKE and oxaliplatin in inducing ROS was due to TrxR1 activity inhibition.

BBSKE and oxaliplatin combination inhibits gastric tumor growth in vivo

To evaluate the in vivo effect of the combined treatment, we used a subcutaneous xenograft model of MGC-803 cells in immunodeficient mice and found that 36 mg/kg BBSKE and 5 mg/kg oxaliplatin inhibited the growth of

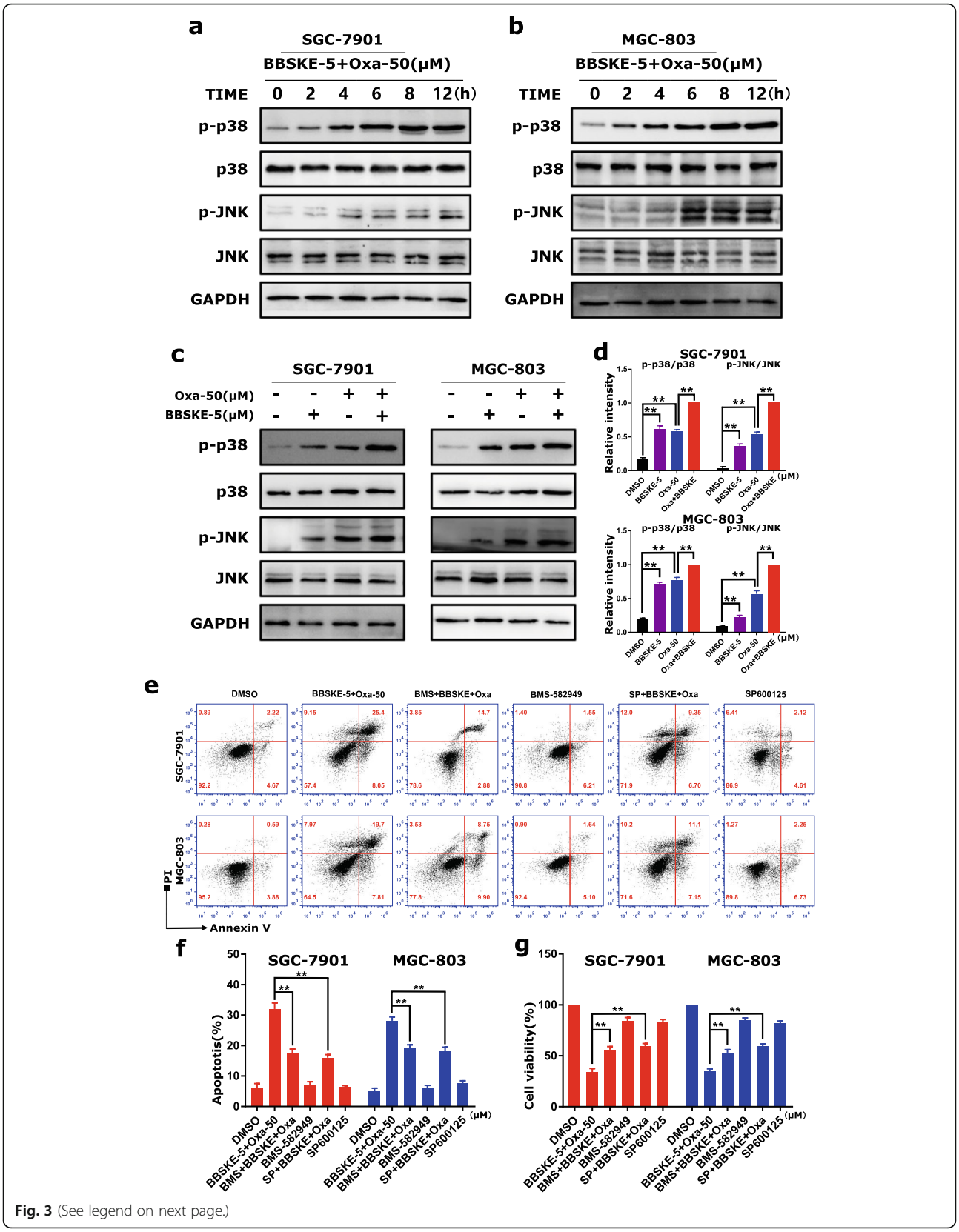

Fig. 3 (See legend on next page.)

(See figure on previous page.)
Fig. 3 Combined treatment of BBSKE and oxaliplatin activated p38 and JNK signaling pathways in gastric cancer cells. **a-b** SGC-7901 and MGC-803 cells were treated with the combined treatment of BBSKE and oxaliplatin for the indicated times, the protein levels of p-p38, p38, p-JNK and JNK were determined by western blot. GAPDH was used as the internal control. **c-d** SGC-7901 and MGC-803 cells were treated with BBSKE and oxaliplatin alone or in combination with the indicated doses. At 24 h after treatment, the protein levels of p-p38, p38, p-JNK and JNK were determined by western blot. **e-g** SGC-7901 and MGC-803 cells were pretreated with BMS-582,949 (10 mM) or SP600125 (20 mM) for 2 h before treated with BBSKE and oxaliplatin for 24 h. The percentage of cell apoptosis was determined by flow cytometry (**e-f**) and the cell viability was determined by CCK8 assay (**g**). Data represent similar results from three independent experiments. (* $p < 0.05$, ** $p < 0.01$)

MGC-803 xenograft effectively after 15 days (Fig. 6a-c). Meanwhile, the combined treatment exhibited stronger inhibitory effects on tumor volume and weight (Fig. 6a-c). Remarkably, the administration of oxaliplatin (5 mg/kg) resulted in a significant weight loss, whereas the combined treatment was well tolerated, suggesting that BBSKE can attenuate the side effects of oxaliplatin (Fig. 6d). We also found that BBSKE treatment remarkably attenuated the decrease of spleen weight evoked by oxaliplatin treatment, and decreased the serum BUN levels induced by oxaliplatin (Additional file 1: Figure S6A-S6C). Mechanistically, TrxR1 activity in tumor tissues was measured by endpoint insulin reduction assay, and the result indicated that combined treatment significantly decreased the activity of TrxR1 (Fig. 6e). Moreover, we found significantly decreased levels of Ki-67 and Bcl-2 and increased levels of p-p38 and p-JNK in tumor tissues from mice treated with BBSKE and oxaliplatin (Fig. 6f). Taken together, these results indicated that BBSKE can synergize the effect of oxaliplatin to inhibit tumor growth in vivo by targeting TrxR1, which was in accordance with the mechanisms in vitro.

BBSKE synergistically increases the cytotoxicity of oxaliplatin in GC Patient-Derived organoids

We used three cases of gastric cancer Patient-Derived organoids (GC-PDO) (Additional file 1: Figure S7) to detect the effect of BBSKE and oxaliplatin. The

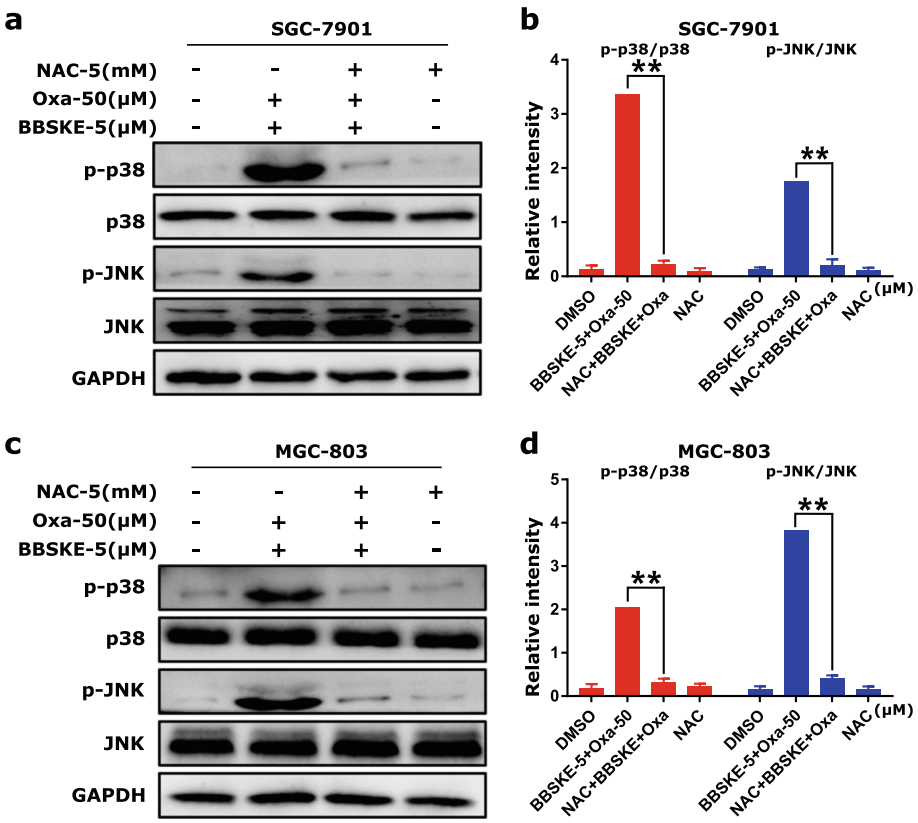

Fig. 4 The activation of p38 and JNK signaling pathways is dependent on intracellular ROS generation. SGC-7901 and MGC-803 cells were pretreated with NAC (5 mM) for 2 h before treated with BBSKE and oxaliplatin. At 12 h after treatment, the protein levels of p-p38, p38, p-JNK and JNK were determined in SGC-7901 (**a-b**) and MGC-803 cells (**c-d**) by western blot. GAPDH was used as the internal control. Data represent similar results from three independent experiments. (* $p < 0.05$, ** $p < 0.01$)

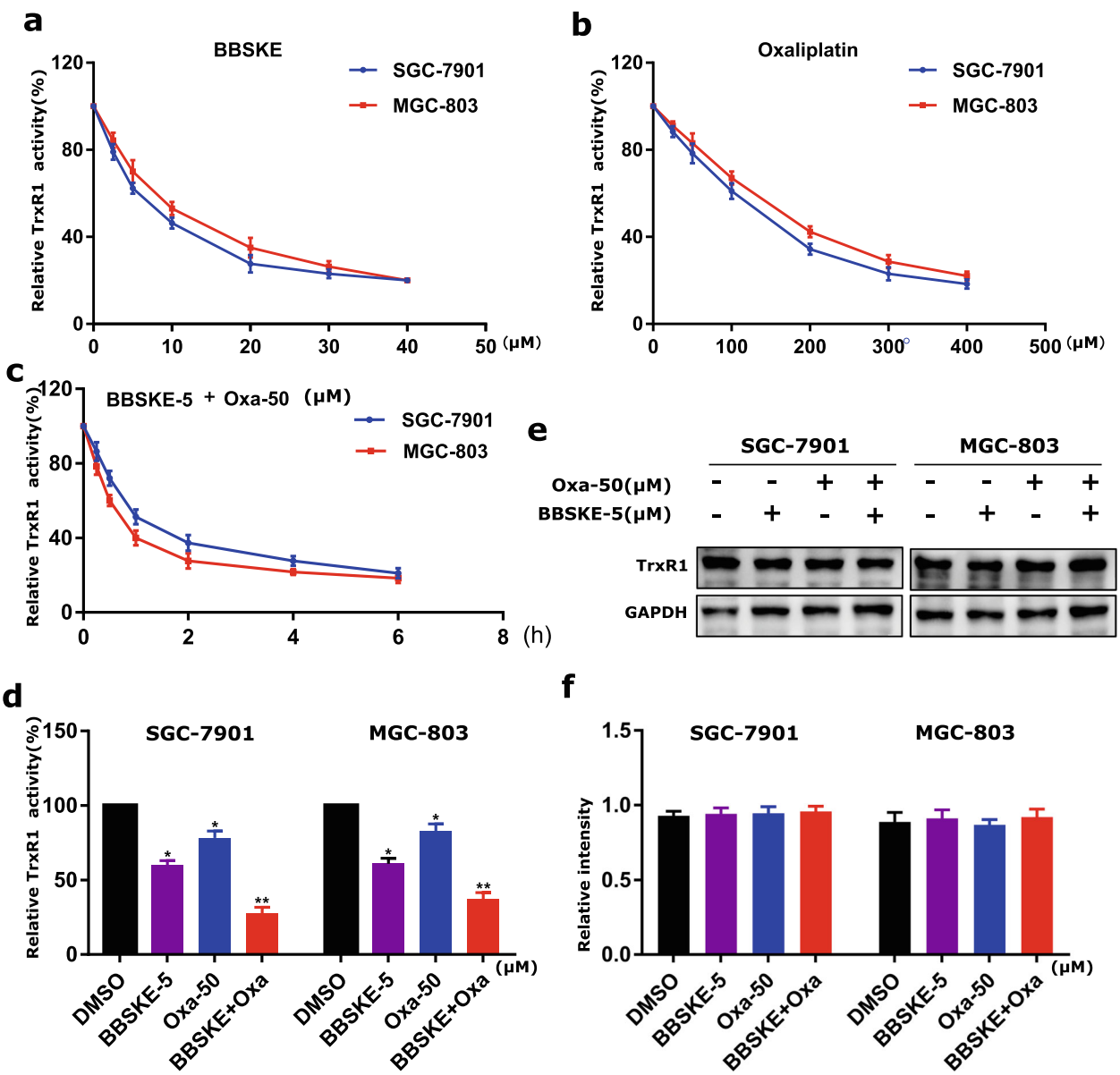

Fig. 5 BBSKE and oxaliplatin combination inhibited TrxR1 activity in gastric cancer cells. TrxR1 activity was measured in SGC-7901 and MGC-803 cells after treated with BBSKE (**a**) or oxaliplatin (**b**). **c** TrxR1 activity was measured in SGC-7901 and MGC-803 cells after treated with the combination of BBSKE (5 μM) and oxaliplatin (50 μM) at the indicated time. **d** SGC-7901 and MGC-803 cells were treated with BBSKE and oxaliplatin alone or in combination with the indicated concentrations. At 2 h after treatment, TrxR1 activity was measured by the endpoint insulin reduction assay. **e-f** SGC-7901 and MGC-803 cells were treated with BBSKE and oxaliplatin alone or in combination with the indicated concentrations. At 12 h after treatment, the TrxR1 expression was determined by western blot. Data represent similar results from three independent experiments. (* $p < 0.05$, ** $p < 0.01$)

morphological images showed that the combined treatment dramatically inhibited the growth of GC-PDO compared with the treatment of BBSKE and oxaliplatin alone (Fig. 7a). We then detected the apoptosis and viability of GC-PDO by flow cytometry and the results showed that the combined treatment significantly induced the apoptosis (Fig. 7b-c) and inhibited PDO viability (Fig. 7d). In addition, we detected the ROS level and TrxR1 activity in GC-PDO and found that ROS level was enhanced by the combined treatment (Fig. 7e), while the TrxR1 activity was inhibited significantly (Fig. 7f). These results observed in GC-PDO were consistent with in gastric cancer cells.

Discussion

The use of conventional chemotherapeutic drugs, including oxaliplatin, is limited due to toxicities and drug resistance. Moreover, its anticancer effects are optimized

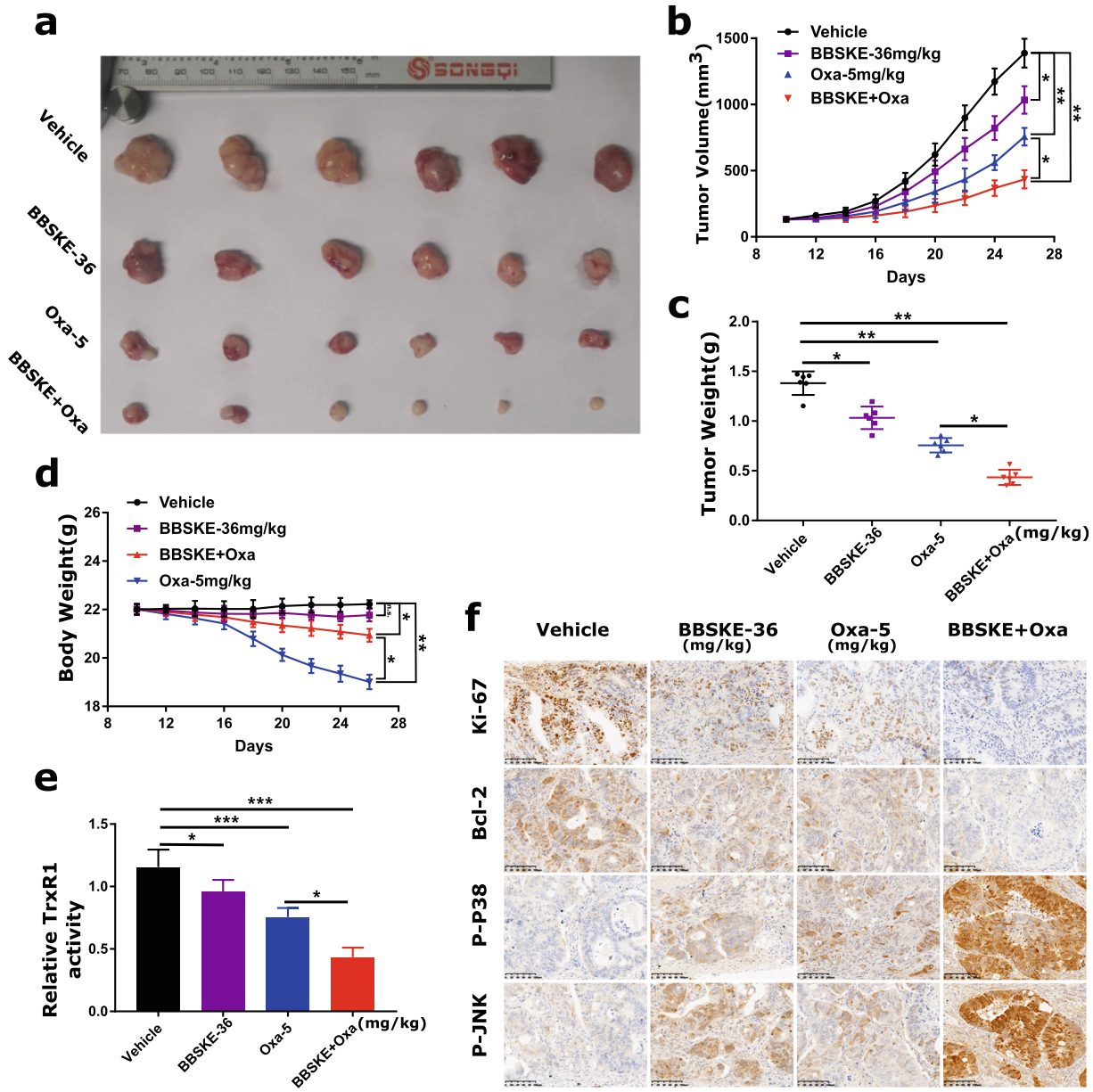

Fig. 6 BBSKE and oxaliplatin combination inhibited SGC-7901 xenograft tumor growth in vivo with decreased TrxR1 activity. **a-d** The combined treatment of BBSKE and oxaliplatin significantly inhibited tumor growth in xenograft nude mice with decreased tumor volume (**b**), tumor weight (**c**) and body weight (**d**). **e** The tumor tissues were lysed and protein was used to determine the TrxR1 activity by using the endpoint insulin reduction assay. **f** The expression levels of Ki-67, Bcl-2, p-p38 and p-JNK proteins in tumor tissues were analyzed by immunohistochemical analysis. Data represent similar results from three independent experiments. (* $p < 0.05$, ** $p < 0.01$, n.s., not significant)

when it is administered in combination with other anticancer agents, such as 5-fluorouracil [42] and S-1 [43, 44].

A study in 2010 already showed the synergistic inhibition of A549 tumor cell growth in vivo by ethaselen and cisplatin combination therapy [45]. It also has been shown that alkaloid piperlongumine, a ROS-inducing agent potentiates the activity of oxaliplatin in gastric cancer [46]. Although the enhanced oxidative damages can potentiate the anticancer activity, they will also likely enhance the oxidative neurotoxicity of oxaliplatin. It has been shown previously that regulation of TrxR1 is a major event in the adverse effects of platinum drugs in kidneys [47]. Another study demonstrated that a specific thioredoxin reductase1(TXNRD1) inhibitor called (TRi-1) can yield anticancer efficacy without overt systemic toxicity [48]. Our previous study has suggested that BBSKE induced growth inhibition and apoptosis in

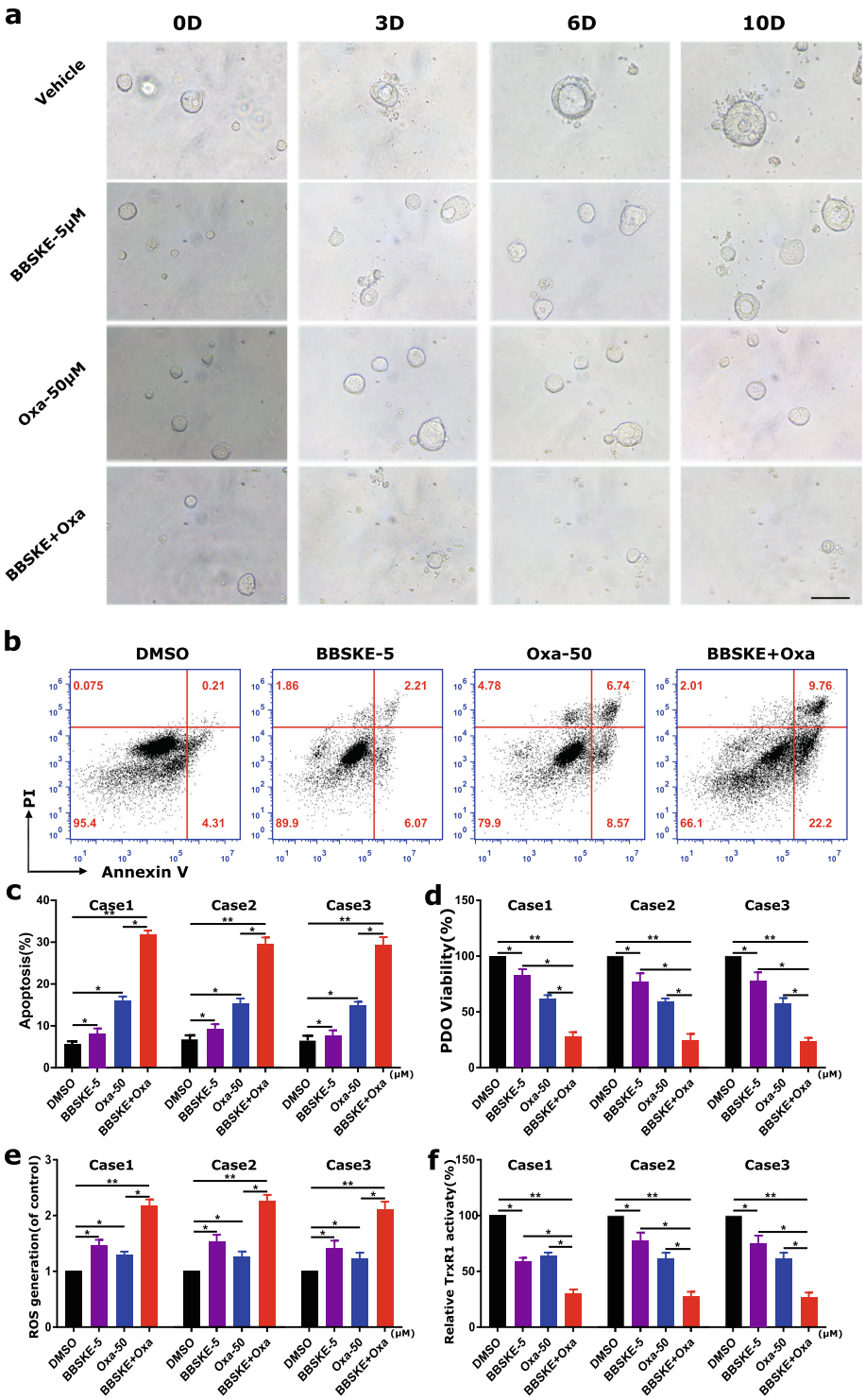

Fig. 7 BBSKE and oxaliplatin combination inhibited GC-PDO growth with increased apoptosis and decreased TrxR1 activity. **a** Representative morphology of GC-PDO treated with BBSKE and oxaliplatin alone or in combination (scale bars, 20 μm). (b-e) GC-PDO were pretreated with BBSKE and oxaliplatin alone or in combination for 24 h. The percentage of cell apoptosis was determined by flow cytometry (**b**) and the percentage of apoptotic cells was calculated (**c**). The cell viability was determined by CCK8 assay (**d**) and the TrxR1 activity was measured by endpoint insulin reduction assay (**e**). Data represent similar results from three independent experiments. (* $p < 0.05$, ** $p < 0.01$)

gastric cancer [32]. In the present study, we investigated the response of human gastric cancer cells to the combined treatment of BBSKE and oxaliplatin. Our results showed that the enhanced inhibitory effect of BBSKE and oxaliplatin on gastric cancer cell growth was mediated through inhibiting TrxR1 activity. By inhibiting TrxR1 activity, BBSKE combined with oxaliplatin markedly induced the production of ROS, activated p38 and JNK signaling pathways, and eventually induced apoptosis of gastric cancer cells (Fig. 8). In vivo, we found that BBSKE combined with oxaliplatin exhibited a synergistic inhibitory effect on gastric tumor growth, and effectively reduced the activity of TrxR1 in tumor tissues, which was consistent with the in vitro results.

Given that by inhibiting TrxR1 activity and increasing intracellular ROS, BBSKE induces a lethal endoplasmic reticulum stress and mitochondrial dysfunction in human gastric cancer cells [30]. Hence, we were interested in whether ROS was involved in the synergistic effect of BBSKE and oxaliplatin. The present study showed that BBSKE and oxaliplatin combined treatment resulted in significant increases in ROS levels, and pretreatment with NAC fully reversed the combined treatment-induced ROS generation and apoptosis, suggesting that ROS play a critical role in the synergistic effect of BBSKE and oxaliplatin. By inducing ROS generation and oxidative stress, the combined treatment concomitantly activated p38 and JNK signaling pathways, as indicated by phosphorylation of both p38 and JNK. In addition, we found that BMS-582,949 or SP600125 could partially attenuate the combined treatment-induced cell growth inhibition and apoptosis, suggesting that activation of

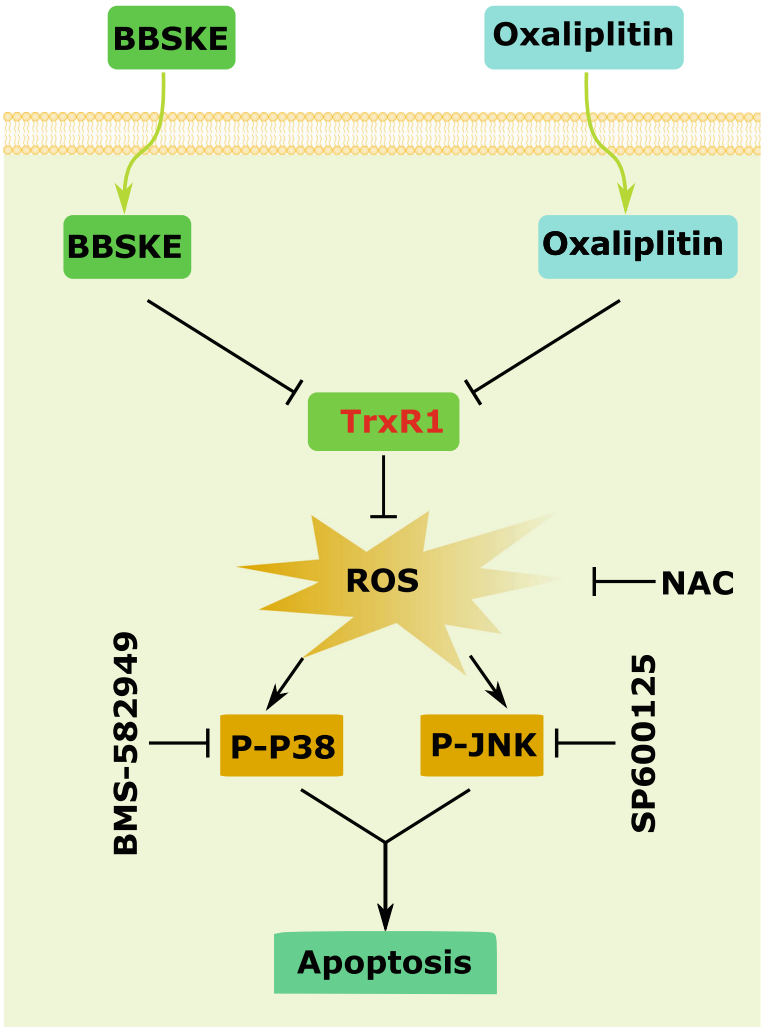

Fig. 8 Schematic illustration of the main findings of the present study

the p38 and JNK signaling pathways is essential for the effect of the combined treatment. Furthermore, we found that pretreatment with NAC markedly reversed the combined treatment-induced phosphorylation of p38 and JNK in both SGC-7901 and MGC-803 cells, suggesting that the activation of p38 and JNK signaling pathways is due to accumulation of intracellular ROS.

The combination of BBSKE and oxaliplatin resulted in significant increases in ROS levels and accumulating evidence indicates that intracellular ROS levels may be increased by TrxR1 inhibition [40, 47]. Using the endpoint insulin reduction assay to quantify inhibition of TrxR1 activity, we found that TrxR1 activity in cell lysates was decreased with increasing BBSKE concentration. Accordingly, we found that TrxR1 activity in gastric cancer cells was decreased after combined BBSKE and oxaliplatin treatment. Interestingly, we observed that the TrxR1 activity was also significantly inhibited by oxaliplatin treatment, which is consistent with previous observations [49].

As organoid has also been shown to be a good model to determine the optimal drugs for the patients.[23–27]. Our study based on GC-PDO exhibited similar effect as in GC cells and in vivo model. The combination treatment significantly inhibited the growth and viability and resulted in significant increases in ROS levels and apoptosis rate of the three cases of GC Patient-Derived organoids. The endpoint insulin reduction assay held on that comparing with BBSKE or oxaliplatin, their co-treatment significantly inhibited TrxR1 activity of GC-PDO.

Conclusions

In conclusion, we found that BBSKE synergized the antitumor effect of oxaliplatin by inhibiting TrxR1 activity and demonstrated that the combined treatment induced apoptotic cell death through ROS-mediated p38 and JNK signaling pathways. These findings provide new insights into the molecular mechanisms by which BBSKE synergized with oxaliplatin and suggest that such a combinatorial treatment might potentially become a more effective way in gastric cancer therapy. Further investigations about the clinical significance of this combination therapy are needed.

Abbreviations

CI: Combination index; DAB: 3,3′-diaminobenzidine; GC-PDO:gastric cancer Patient-Derived organoids; NAC: N-acetyl-L-cysteine; ROS: Reactive oxygen species; Sec: Selenocysteine; TrxR1: Thioredoxin reductase 1

Supplementary Information

The online version contains supplementary material available at https://doi.org/10.1186/s13046-021-02052-z.

Additional file 1: Figure S1. The planar structure of BBSKE. **Figure S2.** Effects of BBSKE on cellular proliferation. **Figure S3.** Pretreatment with GSH markedly attenuated the combined treatment-induced cell growth inhibition in gastric cancer cells. **Figure S4.** The inhibiting efficiencies of p-p38 and p-JNK by BMS-582949 and SP600125 respectively. **Figure S5.** Molecular docking of BBSKE with TrxR1 protein was carried out with the docking software. **Figure S6.** BBSKE reduced the toxicity of cisplatin in *vivo*. **Figure S7.** The morphology of 3 cases of successful established human gastric cancer organoids (hGCO1-3) under white field microscope.

Acknowledgements

Thank the Department of Chem-Biology, School of Pharmaceutical Sciences, Peking University, China, for providing the BBSKE.

Authors' contributions

HZ, CZ, MH designed the research. HZ, JW, HL, YZ, WC, WW, CW, SC performed the research. CZ, YH and JY analyzed the data and wrote the paper. All authors read and approved the final manuscript.

Funding

This study was supported by the Sanming Project of Medicine in Shenzhen (No. SZSM201911010), the National Natural Science Foundation of China (No.82073148), Special Project for sustainable Development, Shenzhen Science and Technology Innovation Commission2020(No. KCXFZ202002011010593), Shenzhen Key Medical Discipline Construction Fund (No. SZXK016),the Research Foundation of Guangzhou Bureau of Science and Technology, and Natural Science Foundation of Guangdong province (No.2015A030312014).

Availability of data and materials

All data generated or analysed during the present study are included in this published article.

Declarations

Ethics approval and consent to participate

The current study was performed with approval from the Ethics Committee of The Seventh Affiliated Hospital, Sun Yat-sen University. All patients provided written informed consent. The animal experiments was performed under the approval of committee on the Ethics of Animal Experiments of The Seventh Affiliated Hospital, Sun Yat-sen University.

Consent for publication

All authors have agreed to publish this manuscript.

Competing interests

The authors declare that they have no competing interests.

Author details

[1]Digestive Diseases Center, The Seventh Affiliated Hospital, Sun Yat-sen University, 518107 Shenzhen, Guangdong, China. [2]Department of Gastrointestinal Surgery, The First Affiliated Hospital, Sun Yat-sen University, 510080 Guangzhou, Guangdong, China. [3]Clinical Research Center, The Seventh Affiliated Hospital, Sun Yat-sen University, 518107 Shenzhen, Guangdong, China. [4]Department of Pathology, The Seventh Affiliated Hospital, Sun Yat-Sen University, 518107 Shenzhen, Guangdong, China.

Received: 4 November 2020 Accepted: 7 February 2021
Published online: 19 August 2021

References

1. Siegel RL, Miller KD, Jemal A. Cancer statistics, 2018. CA Cancer J Clin. 2018; 68:7–30.
2. Chen W, Zheng R, Baade PD, Zhang S, Zeng H, Bray F, Jemal A, Yu XQ, He J. Cancer statistics in China 2015. CA Cancer J Clin. 2016;66:115–32.
3. Van Cutsem E, Sagaert X, Topal B, Haustermans K, Prenen H. Gastric cancer. Lancet. 2016;388:2654–64.
4. Smyth EC, Verheij M, Allum W, Cunningham D, Cervantes A, Arnold D. Gastric cancer: ESMO clinical practice guidelines for diagnosis, treatment and follow-up. Ann Oncol. 2016;27:v38–49.
5. Shitara K, Chin K, Yoshikawa T, Katai H, Terashima M, Ito S, Hirao M, Yoshida K, Oki E, Sasako M, Emi Y, Tsujinaka T. Phase II study of adjuvant

chemotherapy of S-1 plus oxaliplatin for patients with stage III gastric cancer after D2 gastrectomy. Gastric Cancer. 2017;20:175–81.
6. Noh SH, Park SR, Yang HK, Chung HC, Chung IJ, Kim SW, Kim HH, Choi JH, Kim HK, Yu W, Lee JI, Shin DB, Ji J, Chen JS, Lim Y, Ha S, Bang YJ. Adjuvant capecitabine plus oxaliplatin for gastric cancer after D2 gastrectomy (CLASSIC): 5-year follow-up of an open-label, randomised phase 3 trial. Lancet Oncol. 2014;15:1389–96.
7. Bang YJ, Kim YW, Yang HK, Chung HC, Park YK, Lee KH, Lee KW, Kim YH, Noh SI, Cho JY, Mok YJ, Ji J, Yeh TS, Button P, Sirzen F, Noh SH. Adjuvant capecitabine and oxaliplatin for gastric cancer after D2 gastrectomy (CLASSIC): a phase 3 open-label, randomised controlled trial. Lancet. 2012; 379:315–21.
8. Gamelin E, Gamelin L, Bossi L, Quasthoff S. Clinical aspects and molecular basis of oxaliplatin neurotoxicity: Current management and development of preventive measures. Sem Oncol. 2002;29:21–33.
9. Das M. Neoadjuvant chemotherapy: survival benefit in gastric cancer. Lancet Oncol. 2017;18:e307.
10. Mullen JT, Ryan DP. Neoadjuvant chemotherapy for gastric cancer: what are we trying to accomplish? Ann Surg Oncol. 2014;21:13–5.
11. Cebula M, Schmidt EE, Arner ES. TrxR1 as a potent regulator of the Nrf2-Keap1 response system. Antioxid Redox Signal. 2015;23:823–53.
12. Esen H, Erdi F, Kaya B, Feyzioglu B, Keskin F, Demir LS. Tissue thioredoxin reductase-1 expression in astrocytomas of different grades. J Neuro-Oncol. 2015;121:451–8.
13. Zhang W, Zheng X, Wang X. Oxidative stress measured by thioredoxin reductase level as potential biomarker for prostate cancer. Am J Cancer Res. 2015;5:2788–98.
14. Stafford WC, Peng X, Olofsson MH, Zhang X, Luci DK, Lu L, Cheng Q, Tresaugues L, Dexheimer TS, Coussens NP, Augsten M, Ahlzen HM, Orwar O, Ostman A, Stone-Elander S, Maloney DJ, Jadhav A, Simeonov A, Linder S, Arner ESJ. Irreversible inhibition of cytosolic thioredoxin reductase 1as a mechanistic basis for anticancer therapy. Sci Transl Med. 2018;10:1–13.
15. Zheng X, Ma W, Sun R, Yin H, Lin F, Liu Y, Xu W, Zeng H. Butaselen prevents hepatocarcinogenesis and progression through inhibiting thioredoxin reductase activity. Redox Biol. 2018;14:237–49.
16. Raninga PV, Di Trapani G, Vuckovic S, Tonissen KF. TrxR1inhibition overcomes both hypoxia-induced and acquired bortezomib resistance in multiple myeloma through NF-small ka,cyrillicbeta inhibition. Cell Cycle. 2016;15:559–72.
17. Fan C, Zheng W, Fu X, Li X, Wong YS, Chen T. Enhancement of auranofin-induced lung cancer cell apoptosis by selenocystine, a natural inhibitor of TrxR1 in vitro and in vivo. Cell Death Dis. 2014;5:e1191.
18. Cai W, Zhang L, Song Y, Wang B, Zhang B, Cui X, Hu G, Wu YLiu,J, Fang J. Small molecule inhibitors of mammalian thioredoxin reductase. Free Rad Biol Med. 2012;52:257–65.
19. Fiskus W, Saba N, Shen M, Ghias M, Liu J, Gupta SD, Chauhan L, Rao R, Gunewardena S, Schorno K, Austin CP, Maddocks K, Byrd J, Melnick A, Huang P, Wiestner A. K.N.Bhalla, Auranofin induces lethal oxidative and endoplasmic reticulum stress and exerts potent preclinical activity against chronic lymphocytic leukemia. Cancer Res. 2014;74:2520–32.
20. Liu Y, Duan D, Yao J, Zhang B, Peng S, Ma H, Song Y. J. Fang,Dithiaarsanes induce oxidative stress-mediated apoptosis in HL-60 cells by selectively targeting thioredoxin reductase. J Med Chem. 2014;57:5203–11.
21. Steele NG, Chakrabarti J, Wang J, et al. An organoid-based preclinical model of human gastric cancer. Cell Mol Gastroenterol Hepatol. 2019;7:161–84.
22. Czerniecki SM, Cruz NM, Harder JL, et al. High-throughput screening enhances kidney organoid differentiation from human pluripotent stem cells and enables automated multidimensional phenotyping. Cell Stem Cell. 2018;22(6):929–40.e924.
23. Llanos-Chea A, Citorik RJ, Nickerson KP, et al. Bacteriophage therapy testing against shigella flexneri in a novel human intestinal organoid-derived infection model. J Pediatr Gastroenterol Nutr. 2019;68:509–16.
24. Lee SH, Hu W, Matulay JT, et al. Tumor evolution and drug response in patient-derived organoid models of bladder cancer. Cell. 2018;173:515–28.e517.
25. Nuciforo S, Fofana I, Matter MS, et al. Organoid models of human liver cancers derived from tumor needle biopsies. Cell Rep. 2018;24:1363–76.
26. Tiriac H, Belleau P, Engle DD, et al. Organoid profiling identifies common responders to chemotherapy in pancreatic cancer. Cancer Discov. 2018;8: 1112–29.
27. Wang Y, Wang L, Zhu Y, Qin J. Human brain organoid-on-a-chip to model prenatal nicotine exposure. Lab Chip. 2018;18:851–60.
28. Drost J, Clevers H. Organoids in cancer research. Nat Rev Cancer. 2018;18(7): 407–18.
29. Xing F, Li S, Ge X, et al. The inhibitory effect of a novel organoselenium compound BBSKE on the tongue cancer Tca8113 in vitro and in vivo. Oral Oncol. 2008;44:963–9.
30. Zhao F, Yan J, Deng S, et al. A thioredoxin reductase inhibitor induces growth inhibition and apoptosis in five cultured human carcinoma cell lines. Cancer Lett. 2006;236:46–53.
31. Xiao X, et al. The anti-tumor effect of nab-paclitaxel proven by patient-derived. Organoids. 2020;13:6017–25.
32. Wu W, Yang Z, Xiao X, An T, Li B, Ouyang J, Li H, Wang C, Zhang Y, Zhang H, He Y. Zhang C.A thioredoxin reductase inhibitorethaselen induces growth inhibition and apoptosis in gastric cancer. J Cancer. 2020;11(10):3013–9.
33. Chou TC. Drug combination studies and their synergy quantification using the Chou-Talalay method. Cancer Res. 2010;70:440–6.
34. Zou P, Xia Y, Ji J, Chen W, Zhang J, Chen X, Rajamanickam V, Chen G, Wang Z, Chen L, Wang Y, Yang S, Liang G. Piperlongumine as a direct TrxR1 inhibitor with suppressive activity against gastric cancer. Cancer Lett. 2016; 375:114–26.
35. Locatelli SL, Cleris L, Stirparo GG, Tartari S, Saba E, Pierdominici M, Malorni W, Carbone A, Anichini A, CarloStella C. BIM upregulation and ROS-dependent necroptosis mediate the antitumor effects of the HDACi Givinostat and Sorafenib in Hodgkin lymphoma cell line xenografts. Leukemia. 2014;28:1861–71.
36. Wang X, Guo Q, Tao L, Zhao L, Chen Y, An T, Chen Z, Fu R. E platinum, a newly synthesized platinum compound, induces apoptosis through ROS-triggered ER stress in gastric carcinoma cells. Mol Carc. 2017;56:218–31.
37. Tang ZH, Cao WX, Su MX, Chen X, Lu JJ. Osimertinib induces autophagy and apoptosis via reactive oxygen species generation in non-small cell lung cancer cells. Toxicol Appl Pharmacol. 2017;321:18–26.
38. Hsieh CC, Papaconstantinou J. Thioredoxin-ASK1 complex levels regulate ROS-mediated p38 MAPK pathway activity in livers of aged and long-lived Snell dwarf mice. FASEB J. 2006;20:259–68.
39. Mantzaris MD, Bellou S, Skiada V, Kitsati N, Fotsis T, Galaris D. Intracellular labile iron determines H2O2-induced apoptotic signaling via sustained activation of ASK1/JNK-p38 axis. Free Radic Biol Med. 2016;97:454–65.
40. Duan D, Zhang J, Yao J, Liu Y, Fang J. Targeting thioredoxin reductase by parthenolide contributes to inducing apoptosis of HeLa cells. J Biol Chem. 2016;291:10021–31.
41. Duan D, Zhang B, Yao J, Liu Y, Fang J. Shikonin targets cytosolic thioredoxin reductase to induce ROS-mediated apoptosis in human promyelocytic leukemia HL-60 cells. Free Radic Biol Med. 2014;70:182–93.
42. Raymond E, Faivre S, Chaney S, Woynarowski J, Cvitkovic E. Cellular and molecular pharmacology of oxaliplatin. Mol Cancer Ther. 2002;1(3):227–35.
43. Koizumi W, Takiuchi H, Yamada Y, Boku N, Fuse N, Muro K, et al. Phase II study of oxaliplatin plus S-1 as first-line treatment for advanced gastric cancer (G-SOX study). Ann Oncol. 2010;21:1001–5.
44. Oh SY, Kwon H-C, Jeong S-H, Joo Y-T, Lee Y-J, hee Cho S,et al. A phase II study of S-1 and oxaliplatin (SOx) combination chemotherapy as a first-line therapy for patients with advanced gastric cancer. Invest New Drugs. 2012;30:350–6.
45. Tan Q, et al. Augmented antitumor effects of combination therapy of cisplatin with ethaselen as a novel thioredoxin reductase inhibitor on human A549 cell in vivo. J Invest New Drugs. 2010;28(3):205–15.
46. Zhang P, et al. Piperlongumine potentiates the antitumor efficacy of oxaliplatin through ROS induction in gastric cancer cells. Cell Oncol. 2019; 42(6):847–60.
47. Cheng P, et al. Inhibition of thioredoxin reductase 1 correlates with platinum-based chemotherapeutic induced tissue injury. J Biochem Pharmacol. 2020;175:113873.
48. Witte AB, Anestal K, Jerremalm E, Ehrsson H, Arner ES. Inhibition of thioredoxin reductase but not of glutathione reductase by the major classes of alkylating and platinum-containing anticancer compounds. Free Radic Biol Med. 2005;39:696–703.
49. Li K, Zheng Q, Chen X, Wang Y, Wang D, Wang J. Isobavachalcone induces ROS-mediated apoptosis via targeting thioredoxin reductase 1 in human prostate cancer PC-3 cells. Oxid Med Cell Longevity. 2018;1915828:1–13.

Publisher's Note